

**A STUDY ON TUNGSTEN-COPPER COMPOSITES PRODUCED VIA  
COMBINATION OF LIQUID PHASE SINTERING AND LIQUID  
INFILTRATION TECHNIQUES**

**by**

**HAFED IBRAHIM IHMIDA AHMED**

**Thesis submitted in fulfillment of the requirements**

**for the degree**

**of Doctor of Philosophy**

**May 2014**

## **ACKNOWLEDGEMENTS**

Alhamdulillah, great thanks to Almighty Allah who granted me health, patience, capability and knowledge to execute this study.

It is my great pleasure to express my sincere gratitude to my main supervisor Prof. Dr. Azizan Bin Aziz and co-supervisor Prof. Dr. Azmi Bin Rahmat for their scientific and moral support, encouragement and guidance throughout this research work. I thank them a lot for their invaluable ideas and remarks which made this study very interesting. I admire deep from my heart their energetic way of working and their brilliant ideas which made possible this research work to cover a vast area. It's a great opportunity to have worked under their supervision.

I offer my sincere thanks and appreciation to management and all the staff member of School of Materials and Mineral Resources Engineering, Universiti Sains Malaysia for offering me an ideal environment to carry out my research work. At the same time, I sincerely express to acknowledge the assistance of the laboratory technical staffs for all their help. I am grateful to my friends, most especially Khalid Abdullah and his family.

Last but definitely not least, I am forever indebted to my and beloved wife and adorable daughters, who had been extremely supportive of me and shouldered the burden. I wish to thank my parents, sisters and brothers for their encouragement and on-going support during the course of my study. I am deeply thankful to my father in law, and my mother in law for their support.

**Hafed Ibrahim**  
**USM, Penang, 2014**

## DEDICATION

*This work is dedicated to my father, Ibrahim Tajouri, for being my biggest fan and my mother, Sukna Kharis, for being my rock and my beloved wife, Sukeina Ebrahim and adorable kids, Hla, Maryam and Rital.*

## TABLE OF CONTENTS

<b>ACKNOWLEDGEMENTS .....</b>	<b>ii</b>
<b>DEDICATION .....</b>	<b>iii</b>
<b>TABLE OF CONTENTS .....</b>	<b>iv</b>
<b>LIST OF TABLES .....</b>	<b>viii</b>
<b>LIST OF FIGURES .....</b>	<b>x</b>
<b>LIST OF ABBREVIATIONS .....</b>	<b>xxii</b>
<b>LIST OF SYMBOLS .....</b>	<b>xxiv</b>
<b>LIST OF PUBLICATIONS .....</b>	<b>xxvi</b>
<b>ABSTRAK .....</b>	<b>xxvii</b>
<b>ABSTRACT.....</b>	<b>xxviii</b>
<b>CHAPTER ONE INTRODUCTION .....</b>	<b>1</b>
1.1 Introduction.....	1
1.2 Tungsten-copper composites .....	2
1.3 Problem statement .....	3
1.4 Objective of the study .....	5
1.5 Scope of the study.....	6
1.6 Arrangement of the thesis .....	7
<b>CHAPTER TWO LITERATURE REVIEW .....</b>	<b>10</b>
2.1 Introduction.....	10
2.2 Metal matrix composites (MMCs).....	10
2.2.1 Tungsten-copper composites materials .....	12
2.3 Powder Metallurgy (PM) .....	14
2.4 Die compaction.....	15
2.5 Wetting angle and Capillary Force .....	17
2.6 Dihedral angle and Contiguity.....	20
2.7 Distortion .....	22

2.8	Sintering categories .....	23
2.8.1	Solid state sintering (SSS).....	24
2.8.2	Liquid phase sintering (LPS) .....	26
2.8.2.1	Initial stage .....	27
2.8.2.2	Intermediate stage .....	29
2.8.2.3	Final stage .....	30
2.9	Enhanced sintering.....	31
2.9.1	Enhanced sintering by mechanical alloying.....	32
2.9.2	Activated sintering by transition metals addition.....	34
2.10	Liquid infiltration process.....	41
2.10.1	Pressure-less infiltration .....	43
2.10.2	Infiltrated W-Cu composites.....	44
2.11	Combination of liquid phase sintering and liquid infiltration .....	47
2.12	Sintering atmosphere .....	49
2.12.1	Hydrogen gas and mixture of hydrogen and argon gas .....	50
2.12.2	Vacuum.....	50
2.13	Material Properties.....	51
2.14	Phase diagrams .....	53
2.15	Properties and Applications of W-Cu Composites.....	55
2.16	Summary.....	58
<b>CHAPTER THREE METHODOLOGY.....</b>		<b>60</b>
3.1	Introduction.....	60
3.2	Raw Materials and their Characterization .....	62
3.3	Preparation of compact powder .....	63
3.3.1	Mixing Powder.....	63
3.3.2	Compaction .....	65
3.3.3	Fabrication of W-Cu green compact .....	66
3.3.3.1	Sintering process of solid-state and liquid phase sintering .....	67
3.3.3.2	Combined LPS and Liquid Infiltration (Cu-Melts infiltration) .....	68
3.4	Density, porosity and densification measurements .....	70
3.5	Microstructure and phase analysis.....	72
3.5.1	Preparation of samples for microanalysis .....	72

3.5.2 FESEM and EDX .....	73
3.5.3 XRD analysis.....	73
3.6 Mechanical and physical properties.....	74
3.6.1 Microhardness .....	74
3.6.2 Electrical resistivity .....	74
3.6.3 Coefficient of thermal expansion (CTE).....	75
<b>CHAPTER FOUR RESULTS AND DISCUSSION .....</b>	<b>77</b>
4.1 Introduction.....	77
4.2 Characterization of the raw materials .....	77
4.2.1 Scanning electron microscopy (SEM) and energy dispersive X- ray (EDX) of the raw materials .....	78
4.2.2 Particle size distribution .....	82
4.3 Consolidation via SSS, LPS and activated sintering .....	84
4.3.1 The solid-state sintering and liquid phase sintering in vacuum furnace.....	85
4.3.2 The transition elements as sintering activator using vacuum furnace.....	90
4.4 The consolidation via Cu-Melt infiltration (Cu-MI) .....	98
4.4.1 The consolidation of W-Cu composites without addition transition elements as sintering activator in vacuum furnace.....	99
4.4.2 The consolidation of W-Cu composites with addition of low concentration of transition elements as sintering activator .....	102
4.4.3 The effect of green compaction pressure and particle size of tungsten on densification and melt penetration of W-Cu sintered compact under vacuum.....	123
4.4.3.1 The effect of compacting methods on consolidation of W-Cu composites.....	133
4.4.4 The consolidation of W-Cu composites using Cu-MI under H <sub>2</sub> gas as protective gas without additives.....	139
4.5 Comparison between fabricating methods and furnace environment on properties of W-Cu sintered compact .....	156
4.5.1 The effect of furnace atmosphere on consolidation of W-Cu composites.....	157

4.5.2 The effect of furnace atmosphere on contact angle of W-Cu composites.....	161
4.5.3 The comparison of density, hardness and microstructure observed for W-Cu sintered compact produced by different fabrication method under pure hydrogen atmosphere .....	163
4.5.4 The comparison of density, hardness and microstructure observed for W-Cu sintered compact produced by different fabrication method under argon/ hydrogen atmosphere .....	167
4.5.5 The comparison of density, hardness and microstructure observation of W-Cu sintered compact produced by different fabrication method under vacuum atmosphere. ....	175
4.6 The comparison of physical properties.....	177
4.6.1 The comparison of electrical resistivity of W-Cu sintered compact produced by different fabrication method .....	177
4.6.2 The comparison of coefficient of thermal expansion (CTE) of W-Cu sintered compact produced by different fabrication method .....	184
<b>CHAPTER FIVE CONCLUSIONS AND RECOMMENDATIONS .....</b>	<b>187</b>
5.1 Conclusions .....	187
5.2 Recommendations.....	189
<b>REFERENCES.....</b>	<b>190</b>

## **APPENDICES**

**Appendix A** Fraction composition and theoretical density calculation of the sintered compact

**Appendix B** XRD reference files

**Appendix C** Microstructure coupled with mapping EDX results

**Appendix D** Publications

## LIST OF TABLES

Table	Caption	Page
Table 2.1:	The reinforced particles in Cu matrix .....	11
Table 2.2:	The tungsten based reinforcement as metal matrix composites.....	13
Table 2.3:	Contamination contents of Fe, Ni, and Cr on W-Cu composite powders .....	33
Table 2.4:	The materials used and their properties .....	52
Table 2.5:	The solubility of the activators (in weight percent) in Cu and W at the sintering temperatures .....	54
Table 2.6:	The most important properties of W-Cu composite materials .....	56
Table 3.1:	Properties of base raw materials used in this study .....	62
Table 3.2:	Properties of additive materials used in this study.....	63
Table 3.3:	The weight fraction of W powder used in this study .....	64
Table 4.1:	The effect of transition elements additives (Fe, Co and Ni) on penetration behaviour of melt copper into green compact of 80 wt.% W-Cu-X wt.% additive (X= 0, 0.5, 1, 2 and 3) as well as the density and properties of sintered compact. ....	105
Table 4.2:	The effect of transition elements additives (Fe, Co and Ni) on penetration behaviour of melt copper into green compact of 80wt.%W-Cu-Xwt.% additive (X= 0.3, 0.5, 1, 2 and 3 wt.%) as well as the density and properties of sintered compact.....	115
Table 4.3:	The effect of Fe addition on penetration behaviour of melt copper into green compact of 80wt.%W-Cu-Xwt.% additive (X= 0.5, 1 and 2 wt.%) as well as the sintered density (SD) and relative density (RD) of sintered compact. ....	118



Table 4.4:	The effect of starting tungsten powder on mass fraction of penetration of melt copper into the W-Cu green compact during sintering process in vacuum produced by Cu-MI method on adding 1 wt.%Fe as sintering activator.....	127
Table 4.5:	The effect of Cu addition on penetration behaviour of melt copper into green compact of W-XCu, (X= 0, 0.5, 1, 2, 3, 5, 11 and 20 wt.%), the sintered density (SD), relative density (RD) and micro-hardness (Hv)of sintered compact. ....	143
Table 4.6:	The sintering and relative density and densification of 80W-Cu sintered compact prepared by Cu-MI as well as LPS at 1150°C and with different furnace environment .....	158
Table 4.7:	The electrical conductivity and relative density of W-Cu sintered compact produced by using different consolidation method under H <sub>2</sub> gas as sintering atmosphere furnace.....	166
Table 4.8:	The relative density, electrical resistivity and electrical conductivity of W-Cu sintered compact produced by two different techniques ( LPS and Cu-MI) at sintering temperature of 1150°C for 2h under H <sub>2</sub> gas as protective furnace environment.....	180
Table 4.9:	The relative density, electrical resistivity and electrical conductivity of W-Cu sintered compact produced by two different techniques ( LPS and Cu-MI) at sintering temperature of 1250°C for 2h under vacuum furnace .....	184
Table 4.10:	The relative density and coefficient of thermal expansion values for W-Cu sintered compact produced by two different techniques ( LPS and Cu-MI) at sintering temperature of 1150°C for 2h under H <sub>2</sub> gas as protective furnace environment.....	186

## LIST OF FIGURES

Figure	Caption	Page
Figure 2.1:	The different types of metal matrix composites .....	12
Figure 2.2:	The main steps in the scheme of powder metallurgy .....	15
Figure 2.3:	A schematic view of the events during die compaction of single and double action pressing .....	16
Figure 2.4:	Wetting behaviour for a liquid on a horizontal plane .....	18
Figure 2.5:	A schematic of two spheres of size $D_1$ and $D_2$ with a connecting liquid bridge. This geometry is used to calculate the capillary force responsible for rearrangement during LPS .....	19
Figure 2.6:	The dihedral angle for a solid-liquid system .....	21
Figure 2.7:	Illustrates different types of sintering .....	24
Figure 2.8:	A schematic diagram showing the densification curve of a powder compact and also the three sintering stages during solid state sintering .....	25
Figure 2.9:	A schematic diagram of the microstructure changes during LPS .....	28
Figure 2.10:	Two-particle model of liquid phase sintering .....	29
Figure 2.11:	A phase diagram for LPS where the ideal combination of composition and temperature gives solid solubility in the liquid (eutectic liquid in this case) with a low solubility of the liquid in the solid. The melting temperature decrease gives a processing temperature benefit.....	35

Figure 2.12: A schematic diagram shows two models with different representations of the sintering of tungsten particles which has been coated with a metallic activator (a) Brophy et al., model (b) Toth and Lockington model .....	36
Figure 2.13: Isothermal section of the Cu-W-Fe system at 1200°C .....	38
Figure 2.14: Process of gas pressure infiltration for the fabrication of MMCs .....	43
Figure 2.15: Streamlined 2D schematic diagram of the Cu-MI process.....	47
Figure 2.16: An equilibrium phase diagram of W-Cu system at 1 atm .....	53
Figure 2.17: An equilibrium phase diagram of Co-W system .....	55
Figure 2.18: An equilibrium phase diagram of Fe-W system .....	56
Figure 3.1: A flowchart outlining the research activities.....	61
Figure 3.2: A schematic diagram of mixing tungsten powder 80wt.% $W_{16\mu m}$ +20wt.% ( $W_{6.34\mu m}$ or $W_{0.9\mu m}$ ).....	64
Figure 3.3: A flow chart of the one step and two steps press procedure.....	66
Figure 3.4: The schematic diagram of temperature time sintering method.....	67
Figure 3.5: Steps of Cu-melts infiltration method. ....	69
Figure 3.6: The four point probe tester. ....	75
Figure 3.7: The samples for CTE test. ....	76
Figure 4.1: The FESEM micrograph coupled with EDX analysis of (a) $W_I$ powder, (b) $W_{II}$ powder, (c) $W_{III}$ powder and (d) Cu powder .....	79
Figure 4.2: The FESEM micrograph coupled with EDX analysis of (a) Ni powder, (b) Co powder and (c) Fe powder.....	80

Figure 4.3:	The FESEM micrograph coupled with EDX of the W-Cu mixed composite powders prepared by (a) one-stage compact (OSC), (b) two-stage compacts (TSC) and (c) and (d) EDX results of two-stage compact process .....	81
Figure 4.4:	The cumulative distribution and density distribution of base element powder: (a) W <sub>I</sub> powder, (b) W <sub>II</sub> powder, (c) W <sub>III</sub> powder and (d) Cu powder .....	83
Figure 4.5:	The cumulative distribution and density distribution of additive element powders: (a) Ni powder, (b) Co powder and (c) Fe powder .....	84
Figure 4.6:	The FESEM micrograph and photos of W-Cu sintered compact produced by solid-state sintering at 1050°C under vacuum (a) 30 wt.% W- Cu, (b) 50 wt.% W-Cu and (c) 80 wt.% W-Cu .....	86
Figure 4.7:	The BSE micrograph and photos of W-Cu sintered compact produced by LPS at 1150°C under vacuum (a) 80W-Cu, (b) 50W-Cu, the lower photo is the sample after polishing and (c) 30W-Cu, the lower photo is the sample after polishing.....	87
Figure 4.8:	The green, sintering and relative density of W-Cu sintered compact produced by SSS at 1050°C with different Cu content .....	89
Figure 4.9:	The FESEM micrograph of 50 wt.% W-Cu sintered compact produced by SSS at 1050°C under vacuum.....	89
Figure 4.10:	The FESEM micrograph of 80W-Cu sintered at 1050°C with different additive types and concentration under vacuum for 2h (a) and (b) 0.5 and 2 wt.% Co respectively, (c) and (d) 0.5 and 2 wt.% Ni and (e) and (f) 0.5 and 2 wt.% Fe respectively.....	91

Figure 4.11: The FESE micrograph of 80W-Cu sintered compact prepared by LPS at 1150°C with different additives and concentration under vacuum for 2h (a) 0 wt.% additives, (b) 0.5 wt.% Fe , (c) and (d) 0.5 and 2 wt.% Ni and, (e) and (f) 0.5 and 2 wt.% Co .....	93
Figure 4.12: The sintered density of 80W-Cu sintered compact produced by SSS and LPS at 1050°C and 1150°C respectively, under vacuum for 2h with different additive types and content .....	94
Figure 4.13: The FESEM micrograph coupled with EDX of 80W-Cu-2 wt.% Co sintered at 1050°C (a) FESEM micrograph, (b) EDX of selected area at edge of W particles, (c) EDX on the W particles and (d) EDX on Cu matrix .....	96
Figure 4.14: The FESEM micrograph coupled with EDX of 80W-Cu -0.5 wt.% Co sintered compact at 1150°C under vacuum for 2h .....	97
Figure 4.15: The photograph on left side and the FESEM micrograph on right side of W-Cu sintered compact without additives under vacuum at 1150°C for 2h by using Cu-melt infiltration technique (a) and (b) 80W-Cu, (c) and (d) 50W-Cu, and, (e) and (f) 30W-Cu.....	101
Figure 4.16: The green, sintering and relative density of W-Cu sintered compact produced by Cu melt infiltration at 1150°C under vacuum with different Cu content .....	102
Figure 4.17: The BSE micrograph of cross section area of W-Cu sintered compact by Cu-MI at 1150°C under vacuum (a) without additives, no infiltration, (b) 2 wt.% Ni, limited infiltration, (c) 2 wt.% Co, completed infiltration and (d) 2 wt.% Fe, completed infiltration .....	104

Figure 4.18: The FESEM micrograph coupled with EDX results from dense side of 77.7W-Cu-0.47Ni sintered compact at 1150°C under vacuum produced by Cu-MI. The tungsten overall mass fraction of 80wt.% W <sub>16μm</sub> + 20wt.% W <sub>6.3μm</sub> was used.....	107
Figure 4.19: The FESEM micrograph coupled with EDX results of 73.4W-Cu-2.7Co sintered compact produced by Cu-MI at 1150°C under vacuum. The tungsten overall mass fraction of 80wt.% W <sub>16μm</sub> + 20wt.% W <sub>6.3μm</sub> was used. The formation of Co-W interdiffusion layer is evident.....	109
Figure 4.20: The BSE micrograph coupled with EDX results of 75.2W-Cu-2.74Fe sintered compact produced by Cu-MI at 1150°C under vacuum and with added 3 wt.% Fe. The tungsten overall mass fraction of 80wt.% W <sub>16μm</sub> + 20wt.% W <sub>6.3μm</sub> was used.....	110
Figure 4.21: The sintering and densification of W-Cu sintered compact produced by Cu-MI at 1150°C under vacuum for 2h with different sort and content of additives .....	112
Figure 4.22: The relative density and hardness of W-Cu sintered compact produced by Cu-MI at 1150°C under vacuum for 2h with different type and content of additives .....	113
Figure 4.23: The BSE micrograph of 72W-Cu-3Co sintered compact coupled with line EDX of 72W-Cu-3Co sintered compact produced by Cu-MI at 1250°C under vacuum, showing the presence of activator, Co, around W particles.....	119
Figure 4.24: The BSE micrograph of 72W-Cu-3Fe sintered compact coupled with line EDX of 72W-Cu-3Fe sintered compact produced by Cu-MI at 1250°C under vacuum, showing the presence of activator, Fe, around W particles .....	120

Figure 4.25: The XRD analysis results of W-Cu-X wt.% Co sintered compact (X=0, 0.3, 0.5, 1, 2, and 3) produced by Cu-MI at 1250°C under vacuum .....	121
Figure 4.26: The XRD analysis results of W-Cu-X wt.% Fe sintered compact (X=0, 0.3, 0.5, 1, 2, and 3) produced by Cu-MI at 1250°C under vacuum .....	122
Figure 4.27: The BSE micrograph of W-Cu sintered compact produced by Cu-MI at 1250°C under vacuum with added 1 wt.% Fe as sintering activator and using different particle distribution of tungsten (a)100 wt.% W <sub>16μm</sub> (TMFW <sub>1</sub> ), (b) 100 wt.% W <sub>6.3μm</sub> (TMFW <sub>2</sub> ), (c) 100wt.% W <sub>0.9μm</sub> (TMFW <sub>3</sub> ), (d) 80 wt.% W <sub>16μm</sub> +20wt.%.W <sub>6.3μm</sub> (TMFW <sub>4</sub> ) and (e) 80wt.% W <sub>16μm</sub> +20wt.%.W <sub>0.9μm</sub> (TMFW <sub>4</sub> ) .....	125
Figure 4.28: The BSE micrograph coupled with EDX results for selected area of W-20.7Cu-0.77Fe sintered compact produced by Cu-MI at 1250°C under vacuum and using particle distribution of tungsten 100 wt.% W <sub>16μm</sub> (TMFW <sub>1</sub> ), (a) high dense area and (b) low dense area .....	126
Figure 4.29: The green density, sintered density, theoretical density and relative density of W-Cu-1Fe sintered compact produced by Cu-MI at 1250°C in vacuum for 2h with different initial tungsten particle size distribution.....	128
Figure 4.30: The relative density and hardness of W-Cu-1Fe sintered compact produced by Cu-MI at 1250°C under vacuum for 2h with different initial tungsten particle size distribution.....	129

Figure 4.31: The BSE micrograph of 78W-Cu sintered compact produced by Cu-MI method at 1200°C under vacuum and using particle distribution of 80wt.% W <sub>16μm</sub> +20wt.% W <sub>0.9μm</sub> (TMWF <sub>5</sub> ) with added 1 wt.% Fe as activator with different compaction pressure, left hand low magnification and right hand high magnification (a) and (b) 150MPa, (c) and (d) 250MPa and (e) and (f) 400MPa .....	131
Figure 4.32: The sintering and densification of 78W-Cu-1Fe sintered compact produced by Cu-MI at 1200°C under vacuum for 2h with different initial pressure and using particle distribution of 80wt.% W <sub>16μm</sub> +20wt.% W <sub>0.9μm</sub> (TMWF <sub>5</sub> ).....	132
Figure 4.33: The relative density and hardness of 78W-Cu-1Fe sintered compact produced by Cu-MI at 1200°C under vacuum for 2h with different initial pressure and using particle distribution of 80wt.% W <sub>16μm</sub> +20wt.% W <sub>0.9μm</sub> (TMWF <sub>5</sub> ).....	133
Figure 4.34: The FESEM micrograph of 73W-Cu-2wt.% Fe sintered compact at 1250°C for 2h under vacuum, (a) one-stage compact(OSC) and (d) two-stage compacts (TSC) .....	135
Figure 4.35: The SEM micrograph coupled with EDX of 73W-Cu-2 wt.% Fe sintered compact at 1250°C under vacuum for 2h .....	136
Figure 4.36: The XRD analysis results of 73W-Cu sintered compact at 1250°C under vacuum for 2h with added Fe as sintering activator produced by one-stage compact (OSC) and two-stage compacts (TSC).....	137
Figure 4.37: The relative density, densification and hardness of 73W-Cu-X wt.% Fe sintered compact produced by Cu-MI and using one-stage compact (OSC) and two-stage compacts (TSC) at 1250°C under vacuum for 2h with different additive content .....	138



- Figure 4.38: The optical microscope and BSE microstructure of W-20 wt.% Cu sintered compacts produced by Cu-MI at 1150°C for 2h and under H<sub>2</sub> gas (a) and (b) optical graphs shows the top and bottom surface of the sintered compact respectively (c) and (d) low and high magnification BSE microstructure, shows the top surface of the sintered compact and (e) and (f) low and high magnification BSE microstructure at edge of the polished sample ..... 142
- Figure 4.39: The optical microscope and BSE microstructure of W-Cu sintered compacts produced by Cu-MI at 1150°C for 2h and under H<sub>2</sub> gas, left side shows the bottom surface of sintered compact (aberrance of residual copper); middle is the top surface of sintered compact and the right side shows microstructure with low magnification of the top surface (a) W-15Cu, (b) W-22Cu and (c) W-30Cu ..... 146
- Figure 4.40: The BSE micrograph of W-Cu composites produced by Cu-MI at 1150°C under H<sub>2</sub> gas (a) W-15Cu, (b) W-18Cu, (c) W-22Cu and (d) W-30Cu. .... 147
- Figure 4.41: The BSE micrograph of W-16Cu sintered compact produced by Cu-MI at 1150°C under H<sub>2</sub> gas, shows the highly clustered fine W particle distribution in Cu matrix (a) low magnification of 1000X, (b) high magnification of 6000X. The segregation of W fine particle around W coarse particles is evident ..... 148

Figure 4.42: The BSE micrographs of a cross section area of W-30Cu sintered compacts prepared by Cu-MI method at 1150°C under H <sub>2</sub> gas (a) 60X magnification BSE microstructure of cross section area, (b) 1000X magnification BSE microstructure of selected area A (top section) (c) 1000X magnification BSE microstructure of selected area B (middle section) and (d) 1000X magnification BSE microstructure of selected area C (bottom section).....	149
Figure 4.43: The BSE micrographs coupled mapping EDX of a cross section area of W-30Cu sintered compacts prepared by Cu-MI method at 1150°C under H <sub>2</sub> gas (a) mapping microstructure and (b) elements peaks result .....	150
Figure 4.44: The BSE micrographs coupled with EDX results of a cross section area of W-30Cu sintered compacts prepared by Cu-MI method at 1150°C under H <sub>2</sub> gas (a) low magnification BSE microstructure, (b) elements peak and (c) EDX results .....	151
Figure 4.45: The FESEM fractured surface micrograph of W-Cu sintered compact at 1150°C under H <sub>2</sub> gas for 2h (a) W-15Cu, (b) W-22Cu and (c) W-30Cu .....	153
Figure 4.46: The FESEM coupled with EDX fractured surface of 70W-Cu sintered compact at 1150°C under H <sub>2</sub> gas for 2h (1), (2), (3), and, (4). EDX results for different selected area .....	154
Figure 4.47: The XRD pattern of W-Cu sintered compact produced by Cu-MI methods at 1150°C under H <sub>2</sub> gas.....	156

Figure 4.48: Shows the FESEM images coupled with EDX scan for the consolidation of W-Cu composite produced by LPS at 1150°C under H <sub>2</sub> gas as furnace atmosphere shows the effect of O <sub>2</sub> content on the tungsten particles (a) the FESEM micrograph coupled with EDX result on selected area A and (b) the FESEM micrograph coupled with EDX result on selected area B.....	159
Figure 4.49: The EDX results of oxygen elements scanned on the vicinity region of tungsten particles of W-20Cu sintered compact prepared by Cu-MI method under different sintering atmospheres. Specimens consolidation under hydrogen atmosphere resulted the lowest oxygen content and highest relative density.....	161
Figure 4.50: The photographs of 80W-Cu sintered compact at 1150°C under different furnace environment via Cu-MI method, (a) under vacuum, (b) under Ar./H <sub>2</sub> gas (95/5 wt.%), (c) under H <sub>2</sub> gas and (d) measuring of contact angle using stereo zoom microscope.....	162
Figure 4.51: The sintering and relative densities of W-13Cu and W-27Cu composites prepared by Cu-MI and LPS under the same conditions .....	164
Figure 4.52: The FESEM micrograph of W-Cu sintered compact: (a) and (b) W-13Cu and W-27Cu prepared by Cu-MI; and (c) and (d) W-13Cu and W-27Cu prepared by LPS .....	165
Figure 4.53: The comparison of hardness of W-13Cu and W-27Cu composites prepared by Cu-MI and LPS methods .....	167
Figure 4.54: The density and densification of W-Cu sintered compact prepared using LPS and Cu-MI methods under Ag./H <sub>2</sub> gas.....	169

Figure 4.55: The FESEM micrographs of a cross section area of sintered compacts of 80W-Cu-1 Ni prepared under same condition by (a) Cu melt infiltration method and (b) Liquid phase sintering technique.....	171
Figure 4.56: The SEM micrographs of 80W-Cu sintered compact under argon/ hydrogen gas as sintering furnace atmosphere at sintering temperature of 1150°C prepared by (a) Cu-MI method and added 1 wt. % Ni, (b) Cu-MI method and free Ni addition , (c) LPS technique and added 1 wt. % Ni and (d) LPS technique and without Ni addition.....	172
Figure 4.57: The XRD pattern of 80W-Cu sintered compact produced by LPS and Cu-MI methods under argon/ hydrogen gas as sintering furnace atmosphere at sintering temperature of 1150°C for 2h .....	173
Figure 4.58: The Microhardness and relative density of 80W-Cu sintered compact prepared LPS and Cu-MI methods under Ar/H <sub>2</sub> gas with and without adding 1 wt.% Ni as sintering activator .....	175
Figure 4.59: The comparison of the relative density and Micro-hardness of W-Cu sintered compact fabricated via different sintered method LPS and Cu-MI methods at 1250°C for 2h under vacuum. The additive content used as activated sintering is in the range of 0 to 0.88 wt.% .....	177
Figure 4.60: The electrical resistivity and electrical conductivity of different W-Cu sintered compact produced by Cu-MI 1150°C for 2h under hydrogen gas as protective furnace environment.....	179

Figure 4.61: The FESEM images of electrical conductivity test samples with different microstructure observation (a) W-27Cu sintered compact produced by Cu-MI method under H<sub>2</sub> gas with flow rate of 5L/min, (b) W-27Cu sintered compact produced by LPS technique under H<sub>2</sub> gas with flow rate of 5L/min and (c) W-27Cu sintered compact produced by LPS method under H<sub>2</sub> gas with flow rate of 2L/min ..... 181

Figure 4.62: The electrical resistivity and electrical conductivity of W-Cu sintered compact prepared by Cu-MI method with different concentration of transition elements as sintering activator under vacuum furnace and sintering temperature of 1250°C ..... 183

## LIST OF ABBREVIATIONS

<b><u>Abbreviation</u></b>	<b><u>Description</u></b>
<i>ASTM</i>	American Standard of Testing Materials
<i>BS</i>	British standard
<i>BSE</i>	Back scattered electron
<i>Cu-MI</i>	Copper-melt infiltration
<i>CTE</i>	Coefficient of Thermal Expansion
<i>EDX</i>	Energy dispersive X-ray
<i>FESEM</i>	Field emission scanning electron microscopy
<i>GB</i>	Grain Boundary
<i>GD</i>	Green density
<i>HIP</i>	Hot Isostatic Pressing
<i>IACS</i>	International annealed copper standard
<i>ICDD</i>	International center for diffraction data
<i>ICSD</i>	Inorganic crystal structure database
<i>LI</i>	Liquid infiltration
<i>LPS</i>	Liquid phase sintering
<i>MA</i>	Mechanical alloying
<i>MIM</i>	Metal injection moulding
<i>MMC</i>	Metal matrix composite
<i>OSC</i>	One-stage compact
<i>PIM</i>	Powder Injection Molding
<i>PM</i>	Phase diagram
<i>PM</i>	Powder metallurgy

<i>R</i>	Resistivity
<i>RD</i>	Relative density
<i>SD</i>	Sintered density
<i>SE</i>	Secondary electron
<i>SEM</i>	Scanning electron microscopy
<i>SSS</i>	Solid-state sintering
<i>TD</i>	Theoretical density
<i>TR</i>	Thermal resistivity
<i>TSC</i>	Two-stage compact
<i>XRD</i>	X-ray diffraction

## LIST OF SYMBOLS

<b><u>Symbol</u></b>	<b><u>Description</u></b>
$\%$	Percentage
$\%IACS$	International annealing copper standard
$\Delta P$	Capillary pressure
$C_{ss}$	Contiguity
$d$	Pore size
$F_{cap}$	Capillary force
$H_v$	Vickers hardness
$L$	Pore length
$N_{sl}$	Solid-liquid intercepts
$P$	Load
$P_a$	Apparent porosity
$R$	Resistivity
$t$	Sintering time
$T$	Temperature
$V$	Volume
$V_a$	Sample volume
$V_{op}$	Volume of open pores
$W_a$	Sample weight
$W_d$	Dry weight
$W_m$	Saturated weight
$W_s$	Suspended weight
$wt.\%$	Weight percentage
$X$	Neck diameter



$\alpha$	Free angle
$\gamma$	Surface energy
$\gamma_{lv}$	Liquid-vapor surface energy
$\gamma_{sl}$	Solid-liquid surface energy
$\gamma_{sv}$	Solid-vapor surface energy
$\theta$	Contact angle
$P_a$	Sample density
$\Phi$	Dihedral angle
$\Psi$	Densification parameter

## LIST OF PUBLICATIONS

1. **Hafed Ibrahim**, Azizan Aziz, Azmi Rahmat, Enhanced liquid-phase sintering of W-Cu composites by liquid infiltration, **International Journal of Refractory Metals and hard Materials**, 2014; 43: 222-226. (ISI)
2. **Hafed Ibrahim**, Azizan Aziz, Azmi Rahmat, Effects of cobalt addition and temperature on microstructure and density of W-25Cu composites prepared via liquid infiltration, **Advanced Materials Research**, 2013; 626: 430-435. (ISI)
3. **Hafed Ibrahim**, Azizan Aziz, Azmi Rahmat, Kahtan S. Mohammed, Comparison of liquid phase sintering and Cu-melt infiltration methods to consolidate 80W-Cu composite using Nickel as sintering activator, **Applied Mechanics and Materials** 2013; 372:34-40. (ISI)
4. **Hafed Ibrahim**, Azizan Aziz, Azmi Rahmat, Densification behavior and hardness evaluation of consolidated W-25Cu composite powder by re-compaction method, International Conference on Advances in Mechanical and Manufacturing Engineering 2013, Kuala Lumpur, Malaysia, 26 – 28 November 2013. Oral presentation.
5. **Hafed Ibrahim**, Azizan Aziz, Azmi Rahmat, Kahtan S. Mohammed, The Effect of Co and Fe on Densification of W-Cu Composites prepared by liquid infiltration, The Asian International Conference on Materials, Minerals, and Polymer 2012, Penang Island, Malaysia, 23 - 24 March 2012. Oral presentation.
6. **Hafed Ibrahim**, Azizan Aziz, Azmi Rahmat, Kahtan S. Mohammed, Comparison of liquid phase sintering and Cu-melt infiltration methods to consolidate 80W-Cu composite using Nickel as sintering activator, The 2<sup>nd</sup> International Conference on Advance Materials Design and Mechanics 2013, Kuala Lumpur , Malaysia, May 17-18, 2013. Oral presentation.
7. **Hafed Ibrahim**, Azizan Aziz, Azmi Rahmat, Effects of cobalt addition and temperature on microstructure and density of W-25Cu composites prepared via liquid infiltration, International Conference on Advanced Material Engineering and Technology 2012, Batu Feringhi, Penang Island, Malaysia, 28-30 November 2012. Oral presentation

# **KAJIAN TERHADAP KOMPOSIT TUNGSTEN-KUPRUM DIHASILKAN MELALUI GABUNGAN TEKNIK PENSINTERAN FASA CECAIR DAN PENYUSUPAN CECAIR**

## **ABSTRAK**

Keterlarutan rendah antara unsur-unsur W dan Cu menjadikannya sukar untuk mencapai ketumpatan penuh menggunakan kaedah pensinteran konvensional. Dalam karya ini satu kaedah yang unik telah dicadangkan untuk membina sistem W- Cu, mencapai sifat komposit yang sangat baik. Kaedah baru yang dicadangkan menggabungkan pensinteran fasa cecair dan penyusupan cecair dan dinamakan sebagai kaedah penyusupan tembaga - kuprum cair (Cu -MI). Serbuk elemen unsur asas tungsten (W) dan tembaga ( Cu) dan unsur-unsur tambahan seperti nikel (Ni ) , kobalt (Co) dan besi (Fe ) telah digunakan dalam kajian ini. Unsur-unsur tambahan telah digunakan sebagai pengaktif pensinteran dalam lingkungan 0.3-3wt.%. serbuk dicampurkan unsur secara manual dalam lesung alumina selama 30 minit untuk menghasilkan serbuk komposit. Selepas itu, serbuk campuran dipadatkan di bawah tekanan yang berbeza (150-650MPa) disinter secara isothermal pada suhu yang berbeza (1050, 1150 dan 1250°C) dan juga atmosfera yang berbeza ( vakum, campuran hidrogen dan gas argon , gas argon tulen dan gas hidrogen tulen ). Dalam pembangunan pendekatan pensinteran, ketumpatan penuh (>99% daripada ketumpatan teori ) padatan tersinter telah dicapai pada suhu pensinteran rendah 1150°C di bawah gas hidrogen sebagai persekitaran relau perlindungan berbanding dengan kepadatan pensinteran rendah (tidak melebihi 89% daripada ketumpatan teori ) padatan tersinter yang sama yang disediakan oleh konvensional pensinteran fasa cecair. Menggunakan gas hidrogen sebagai persekitaran relau perlindungan memberikan hasil yang terbaik berbanding dengan persekitaran relau yang lain. Kekonduksian elektrik dan kekerasan telah dipertingkatkan dengan menggunakan kaedah penyusupan tembaga-cair mencairkan untuk membina W-Cu hijau padat. Tambahan pula, kaedah masukkan Cu-MI telah digunakan untuk mengenal pasti kelebihan berbanding konvensional pensinteran fasa cecair.

# **A STUDY ON TUNGSTEN-COPPER COMPOSITES PRODUCED VIA COMBINATION OF LIQUID PHASE SINTERING AND LIQUID INFILTRATION TECHNIQUES**

## **ABSTRACT**

The low solubility between W and Cu elements makes it difficult to attain full density using the conventional sintering methods. In this work a unique method has been proposed to fabricate the W-Cu system, achieving excellent composite properties. The proposed new method combines the liquid phase sintering and liquid infiltration and is named as the Copper-Melt Infiltration (Cu-MI) method. Base element powders of tungsten (W) and copper (Cu) and the additive elements of nickel (Ni), cobalt (Co) and iron (Fe) were used in this study. The additive elements were used as sintering activator in the range of 0.3-3 wt. %. The elemental powders were mixed manually in alumina mortar for 30 minute to produce composite powders. Thereafter, the mixture powder was compacted under different pressure (150-600MPa) and isothermally sintered at different temperature (1050, 1150 and 1250°C) as well as different atmosphere (vacuum, mixture of hydrogen and argon gas, pure argon gas and pure hydrogen gas). In the development of sintering approach, full density (>99% of theoretical density) of the sintered compact was achieved at low sintering temperature of 1150°C under hydrogen gas as protective furnace environment compared with low sintering density (not more than 89% of theoretical density) of the same sintered compact prepared by conventional liquid phase sintering. Using hydrogen gas as protective furnace environment gave the best outcome compared with others environment furnace. The electrical conductivity and hardness were enhanced using copper-melt infiltration method to fabricate the W-Cu green compact. Furthermore, Cu-MI consolidation method was employed to identify the advantages over conventional liquid phase sintering.

# **CHAPTER ONE**

## **INTRODUCTION**

### **1.1 Introduction**

The 1960s saw a surge in the use of metal matrix composites (MMCs) in many automobile, aerospace and electronic industries owing to their excellent thermal, mechanical and electrical properties. The field of composite materials involves combining two or more phases by subjecting them to some process to arrive at a completely new material having very desirable and attractive properties, not obtainable with the single phase. Composite materials consisting of reinforced (metal or ceramic) and matrix (metal), can also be categorized as MMCs (Chung, 2010).

Recent years have shown some spurt in study related to tungsten based reinforcement as metal matrix composites (Ho, 2008; Qureshi, 2010; Zhou et al., 2011). It is chosen for its good mechanical properties and low thermal expansion coefficient similar to silicon. On account of its low thermal expansion coefficient and high melting point in addition to good wear resistance, tungsten along with high thermal properties of Cu makes tungsten-copper composites suitable in a variety of applications. It has wide applications in electric and electronic applications such as thermal packages (heat sink), electrical appliances at high voltage, electro-discharge machining electrodes, resistance welding electrodes and martial applications as well such as ammunitions, waterfowl shots and kinetic energy penetrator (Hong et al., 2007 and Fan et al., 2012).

## 1.2 Tungsten-copper composites

Tungsten-copper (W-Cu) composites are promising materials for thermal managing applications such as microelectronic devices because of the low thermal expansion coefficient of tungsten and the high thermal conductivity of copper. The combinations of W and Cu elements can also optimize other important alloys properties such as ductility, mechanical strength and wear and corrosion resistance.

The low solubility of W in Cu elements (only  $10^{-7}$ wt.%), makes it difficult to attain full or near density of W-Cu composites using solid-state sintering (SSS), liquid phase sintering (LPS) or/and liquid infiltration (LI) techniques (German et al., 2009; Lu et al., 2001a). The liquid infiltration technique is most widely used for fabrication W-Cu composite. This method is costly than LPS process, because it is carried out in two steps: firstly the W skeleton is prepared with desirable density; thereafter the pores in W skeleton are infiltrated by molten copper. In liquid phase sintering technique, it is difficult to obtain the highly dense W-Cu composites, due to the very low solubility of W in Cu. In order to overcome this problem in W-Cu system, several studies have shown that, adding low concentration of transition elements (group VIII) leads to improvement in the wettability and decreases the sintering temperature for W-Cu system (Moon and Lee, 1979; Johnson and German, 1993 and Mohammed et al., 2013). Additional studies have demonstrated the use of mechanical alloying for enhancing the sinterability of W-Cu composites by decreasing W particle distribution (Kim and Moon, 1998; Raghu et al., 2001 and Mohammed et al., 2013). Some studies have employed more advance techniques of altering the surface morphology and the wettability of the hard metal (W) by coating

thin film of Ni on the surface morphology of W particles prior to sintering (Zangeneh-Madar et al., 2009 and Chen et al., 2010).

The full density of the sintered parts is amongst the vital factors deciding the mechanical and physical properties of the sintered compacts which are generally fabricated by technology of powder metallurgy. The sintered compacts produced had low density, and the mean porosity level in the sintered compact was high. Besides the mechanical and electrical properties of the sintered compact such as electrical and thermal conductivity, flexural strength and hardness were not satisfactory. The main objective of all of these processes was to achieve a full or near full dense and homogenous microstructure of W-Cu composites. Unfortunately, none of these techniques were successful in achieving full density of sintering W-Cu system. On the other hand, it culminated in disastrous mechanical and/ or electrical properties of the sintered compact such as reduction in strength and electrical conductivity and coefficient of thermal expansion.

### **1.3 Problem statement**

Several attempts have been made to study the sintering and densification of W-Cu composites. Tungsten and copper elements are difficult to cast due to the high melting point of W (3410°C). These two elements exhibit very low solubility in both solid and liquid phase as per the equilibrium phase diagram. This limitation eliminates the use of conventional techniques to enhance the sinterability and densification of W-Cu system. The low solubility between W and Cu makes the densification of W-Cu composites by solution re-precipitation to be negligibly small. Consequently, densification can be attributed to either rearrangement or solid-state

sintering. This means that, during heating stage and at temperature higher than melting point of copper, the copper starts to melt and produce a thin film of liquid surrounding the W phase. The presence of a liquid phase noticeably reduces the friction of inter-particles and also enhances particle rearrangement.

The very low solubility between W and Cu elements makes it difficult to attain full density by using conventional sintering method (liquid phase sintering and /or liquid infiltration). Moreover, the big difference in density between W ( $19.3\text{g/cm}^3$ ) and Cu ( $8.9\text{g/cm}^3$ ) lead to distortion and slumping during sintering process. Key factors for better filling of pores and particle rearrangement is the volume fraction of soft metal (Cu element) (Wu et al., 2003). Consequently, it is very difficult to obtain the net shape and full densification using high volume fraction of Cu under sintering temperature more than melting point of copper. Besides, the higher melting point of W ( $3410^\circ\text{C}$ ) compared to the Cu having a melting point of only  $1084^\circ\text{C}$  is an additional constraint in attaining high densification at temperature close to melting point of Cu. This is because, the sintering temperature (above  $1300^\circ\text{C}$ ) leads to evaporation and weight loss of the Cu element especially under vacuum furnace (Ozer et al., 2007). Considering all the limitations associated with W and Cu elements, the conventional sintering techniques are not useful in achieving full density or net full density. Many methods have been tried to improve the sintered density of W-Cu composites, such as liquid phase sintering, liquid infiltration, combined the last two technique with mechanical alloy or /and added low concentration of transition elements (Ni, Co and Fe) as sintering activators with not much success. In this work, a novel method which combines the two techniques (liquid phase sintering and liquid infiltration and named hereinafter as copper-melt



infiltration (Cu-MI)) was developed and used to improve the densification and properties of W-Cu system with and without added low concentration of transition elements as sintering activator. This study is a contribution in this direction, and addresses the limitations associated with previous fabrication methods.

#### **1.4 Objective of the study**

The present research work aimed to develop a technique of consolidation tungsten-copper composite materials. Combination of liquid phase sintering (LPS) and liquid infiltration (LI) named as copper melt infiltration (Cu-MI) was used to fabricate W-Cu composite. The specific objectives are:

- i. To study the effects of fabrication method (solid-state sintering, liquid phase sintering and addition of sintering activator such as Co, Ni and Fe) to the properties of W-Cu sintered compact composites.
- ii. To develop a unique sintering approach combining the liquid phase sintering and liquid infiltration techniques, named hereinafter as copper melt infiltration (Cu-MI) to fabricate W-Cu sintered compact and study the effect of adding of low concentration of transition elements, compact pressure, tungsten particle size and furnace environment on densification of W-Cu composite.
- iii. To investigate the effect of two stage single compact process on densification and properties of W-Cu-Fe sintered compact produced by Cu-MI and at sintering temperature of 1250°C under vacuum furnace.

- iv. To evaluate microstructure, density mechanical and physical properties of W-Cu composites fabricated via the various technique and parameter above.

### **1.5 Scope of the study**

The scope of the present study covers the consolidation of W-Cu composites produced by different sintering techniques, such as solid-state sintering, liquid phase sintering, and combined liquid phase sintering and liquid infiltration-copper-melt infiltration (Cu-MI), along with addition of low concentration of transition elements as sintering activator. Basically, the idea was to develop a suitable method to overcome the limitations of conventional techniques and attain full density of W-Cu sintered compact. The application of the new sintering approach (Cu-MI) and optimization of the sintering parameter led to a significant enhancement in the densification of W-Cu system. Besides, the W-Cu sintered compact produced very high homogenous microstructure and fully dense structures. The sintering techniques were carried out under different sintering temperature and furnace environment. These sintering techniques include:

- Solid state sintering at sintering temperature of 1050°C (less than melting point of copper 1084°C) and liquid phase sintering at sintering temperature of 1150°C and 1250°C (higher than melting point of copper 1084°C).
- Combining LPS and LI techniques at sintering temperature of 1150°C and 1250°C under different atmosphere furnace.

- Activation sintering by adding low concentration of transition element (Ni, Co and Fe) to enhance the solubility between W and Cu elements.

The W-Cu sintered compacts were characterized by means of density, hardness, electrical conductivity, wear resistance and coefficient of thermal expansion. Change in microstructure, density, hardness and physical properties due to use of different sintering methods were evaluated according to compaction, type and content of additives, type of furnace environment. Improved properties of W-Cu sintered compacts produced by Cu-MI method were compared with the same composition prepared by LPS technique; both techniques were prepared in same sintering condition.

This attempt is aimed to economize the fabrication of W-Cu composites. It is expected that this new fabrication method will help lower the cost of energy requirement in manufacturing W-Cu composites when compared to the conventional infiltration techniques.

## **1.6 Arrangement of the thesis**

This thesis consists of five chapters; each of them represents an integral part of the main work that is sequentially arranged. The content of each chapter is given in brief as follows.

### **Chapter 1 (Introduction)**

This chapter presents an overview of the densification method for producing metal matrix composite and W-Cu composites. It also describes the possibility of

addition of low concentration of transition elements as sintering activator as part of this study. The problem statement, research objectives, scope of the work, and organization of the thesis are also covered in this chapter.

## **Chapter 2 (Literature review)**

This chapter reviews several fabrication methods and sintering behaviour of W-Cu composites related to the present study. It also discusses the various challenges and difficulties in preparation of W-Cu composites and identifies the research gaps from the available literature. Besides, previous studies related to the present work in terms of fabrication method, sintering condition and the results obtained are discussed in detail.

## **Chapter 3 (Materials and methods)**

This chapter lists the materials, and equipment used in this work. The research methodology employed in this study is well presented here. Detailed experimental setup for composites preparation, description of the mixing, compaction and sintering as well as the characterization of the sintered compacts are outlined in this chapter.

## **Chapter 4 (Results and discussion)**

This chapter is main thrust of this thesis as it presents the outcome of the present investigation, interprets and analyzes the obtained results. In order to provide flow of the information, the chapter is divided into six major sections; (i) characterization of the raw materials, (ii) consolidation via SSS; LPS and activated sintering, (iii) consolidation via Cu-melt infiltration (Cu-MI), (iv) effect of furnace

atmosphere, (v) comparison of fabrication methods and furnace environment on properties of W-Cu sintered compact and (vii) comparison of physical properties of the sintered compact produced by different sintering techniques. Moreover, each section also presents the characterization and the densification tests of each the sintered compact. Furthermore, the effects of different sintering parameters are analyzed in detail. Lastly, the chapter includes the results and discussion of the comparison properties of the W-Cu sintered compact prepared by different fabrication method.

## **Chapter 5 (Conclusion and Recommendation)**

This chapter presents the conclusion of the findings of this research and suggests recommendations for future study in the field of metal matrix composite and in the improvement of the densification.

## **CHAPTER TWO**

### **LITERATURE REVIEW**

#### **2.1 Introduction**

This chapter comprehensively reviews all the important and significant previous works on different types of metal matrix composites with particular emphasis on composites of W-Cu. The metal matrix composite of reinforced particle and its matrix phase and composite materials of W-Cu are also sequentially presented. Next, the detailed procedures of powder metallurgy used in the preparation of tungsten copper composites are described. Subsequently, the fabrication techniques of W-Cu composite, process of enhancing the densification of W-Cu composites as well as effect of environmental furnace are explained in detail. The properties of selected materials for this study, application and properties of W-Cu composites are introduced in the final part of this chapter.

#### **2.2 Metal matrix composites (MMCs)**

MMCs consist of at least two physically and chemically dissimilar phases, properly distribution to make available properties not achievable with any individual phases. MMCs consist of reinforcement (metal) and matrix (a metallic alloy or metal); wherein the melting point of reinforcement is higher than matrix. Metal-matrix composites are acquiring importance, because advantage with respect to unreinforced metal and advantages with respect to other composites such as polymer matrix composite.

Briefly, MMCs, particularly the particulate sort, can make available improvements in properties, difficult to achieve using individual phase. The most important properties development by MMCs is mechanical properties (hardness and wear) and thermal properties (thermal expansion coefficient and thermal resistivity). Moreover, good thermal and mechanical properties made the MMCs suitable for a variety of applications such as aerospace, automotive and railway, electronic and thermal management, filamentary superconducting magnets, power conduction and wear-resistance materials. The composite properties depended on phase properties, amount of constituents, particle distribution, particle shape and size. For examples, the combine high strength to weight ratio with excellent stiffness has made materials of carbon fibers suitable for high performance composites (wings, tails and fuselages) in the application of aerospace. More examples for MMCs with copper as the matrix are shown in Table 2.1

Table 2.1: The reinforced particles in Cu matrix

<b>Reinforcement</b>	<b>Reference</b>
<b>TiC</b>	(Rathod et al., 2009)
<b>WC</b>	(Deshpande et al., 2006)
<b>NbC</b>	(Zuhailawati and Yong, 2009)
<b>SiC</b>	(Gan and Gu, 2008)
<b>Al<sub>2</sub>O<sub>3</sub></b>	(Rajkovic et al., 2010)
<b>TaC</b>	(López et al., 2005)
<b>WC, Nano-size</b>	(Yusoff et al., 2011)

In general, based on the matrix categories, composite materials are classified into three groups namely metal matrix, polymer matrix and ceramic matrix. Basically there are three types of metal matrix composites particle reinforced MMCs. The short fiber or whisker reinforced MMCs and continuous fiber or sheet reinforced MMCs are shown in Fig. 2.1. This study is based on hard particles of tungsten reinforced soft metal of copper which is also known as tungsten-copper composite materials.

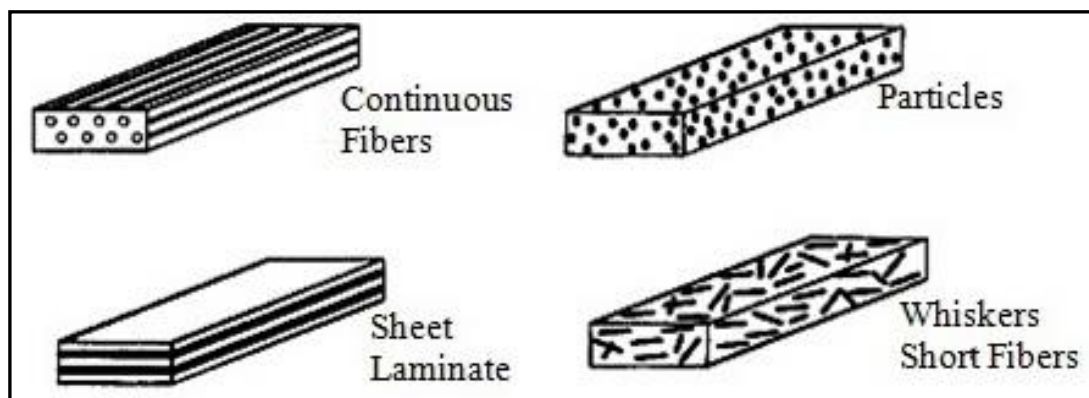


Figure 2.1: The different types of metal matrix composites (Nikhilesh and Krishan, 2006)

### 2.2.1 Tungsten-copper composites materials

In nature, we do not find elements (materials) having two or more phases embedded together naturally via reaction or phase transformations. The field of composite materials involves combining two or more phases by subjecting them to some process to arrive at a completely new material having very desirable and attractive properties, not available with the single phase. It is for this reason composite materials consisting of reinforcing (metal or ceramic) and matrix (metal), can be categorized as MMCs (Chung, 2010).



Recent years have shown some spurt in study related to tungsten based reinforcement in metal matrix composites (Ho, 2008). Metal matrix composite is chosen for its good mechanical properties and low thermal expansion coefficient similar to silicon. Wide-ranging reinforcement of W particles that have been used in general is shown in Table 2.2.

Table 2.2: The tungsten based reinforcement as metal matrix composites

<b>W based Reinforcement</b>	<b>References</b>
W-Cu functionally graded material	(Dorfman, 2002 and Zhou et al., 2011)
W-Ni-Fe tungsten heavy alloy	(Çalışkan et al., 2013 and Mondal et al., 2010a)
W-Ni-Cu tungsten heavy alloy	(Shen et al., 2005 and Jang et al., 2007)
W-Ag composites	(Qureshi, 2010)
W-bronze composites	(Elliott, 2007 and Mohammed et al., 2009)
W-Cu composites	(Selvakumar et al., 2013; Zhou et al., 2013; EL-Hadek et al., 2013; Abbaszadeh et al., 2012; Abyzov et al., 2012 and Hamidiet al., 2011a)

On account of its low thermal expansion coefficient and high melting point in addition to good wear resistance, tungsten along with high thermal properties of Cu makes tungsten-copper composites suitable in a variety of applications. It has wide applications in electric and electronic applications such as thermal packages (heat sink), electrical appliances at high voltage, electro-discharge machining electrodes, resistance welding electrodes and martial applications as well such as ammunitions, waterfowl shots and kinetic energy penetrator. The different tungsten contents in W-Cu systems have unique applications. For example, W-Cu composites containing 80-95 Wt. % tungsten are particularly suitable for electronic packages (heat sink).

Decreasing the W content in the range of 75-50 Wt. % makes it suitable for electrical contact materials and military application such as shaped charge liner and ammunitions (Hong et al., 2007; Fan et al., 2012; Mohammed et al., 2009 and Elliott, 2007). Besides these composite materials can be fabricated using the powder metallurgy technique which involves mixing, compact and sintering processes (German 1984 and Assar, 1998).

### **2.3 Powder Metallurgy (PM)**

Powder metallurgy is the study of processing various kind of metal powder and includes fabrication and conversion of metal powder into useful engineering component. One of the major attractions of P/M is ability to fabricate high quality complex parts to close tolerances in an economic manner. An important characteristic of the powder is its relative high surface area to volume ratio. It is then mixed with other elements such as lubricant and different type of additives. In the beginning, the different type of powders selected are mixed and compacted in order to achieve the shape of the sample. Later heat treatment is applied under suitable condition. In most cases, the powders will be metallic, although in many instances they are combined with other phase ceramics or polymers (Raharijaona et al., 2010). An important characteristic of the powder is its relatively high surface area to volume ratio.

Powder metallurgy is the study of processing various kinds of metal powders and includes the fabrication, characterization, and conversion of metal powders into useful engineering component as shown in Fig 2.2. One of the chief attractions of powder metallurgy is its ability to fabricate high quality complex parts to close

tolerances in an economical manner. In essence, powder metallurgy converts a metal powder with a specific attribute of size, shape, and packing, then converts it into a strong, precise, high performing substance (German, 1984).

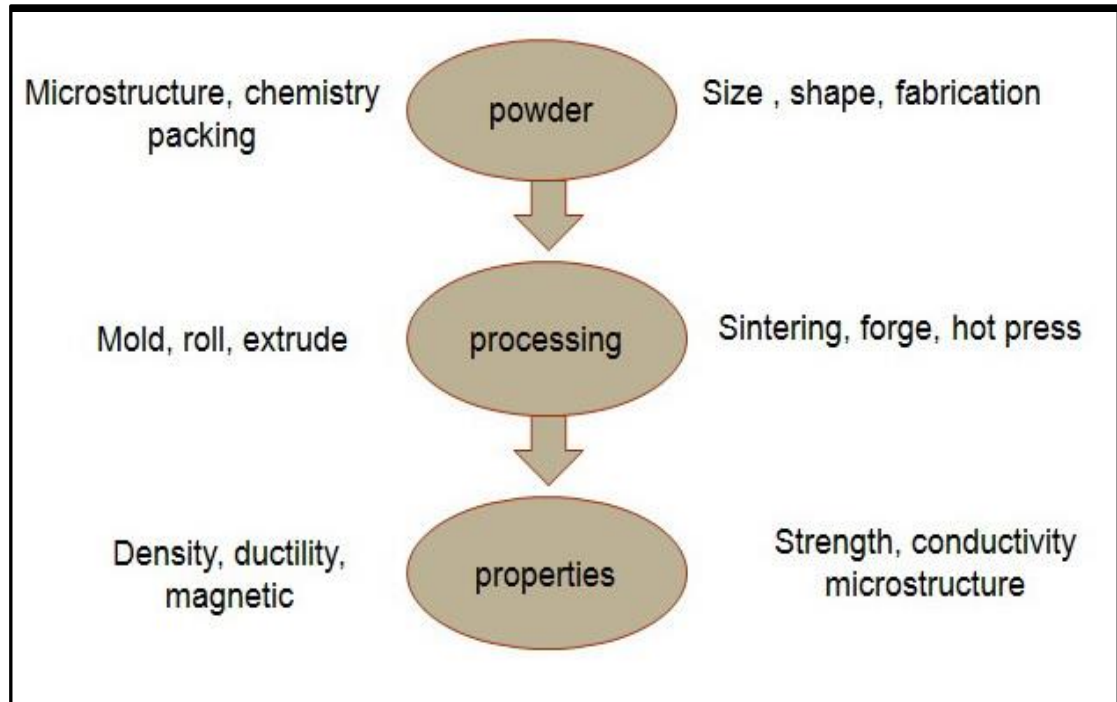


Figure 2.2: The main steps in the scheme of powder metallurgy (German, 1984)

## 2.4 Die compaction

Die compaction of powder relies on pressure technique to develop green strength. The aim of this process is to acquire a very detailed picture of the powder density distribution in the die cavity before, during and after finishing the compaction stroke. This helps to provide precise local stress distribution within the tool and it compacts together with the associated deformations. For handling a sample, the mixed powder must have sufficient strength to produce green compact, but full strength will only be attained after sintering the green compact. Hydraulic presses are usually used up to 100 ton punch loads, and can incorporate complex

tooling kinematics within a single press cycle including rapid advance (closing of the die cavity), medium speed (initial compaction) and slow speed (final compaction).

Fig. 2.3 shows the schematic view of the events during die compaction (single and double action pressing). The compacting techniques used may be characterised by references to the movement of the individual tool elements – upper punch, lower punch and die relative to one another. Pressing within fixed dies can be divided into single action pressing and double action pressing. In the former the lower punch and the die are both stationary. The pressing operation is carried out solely by the upper punch as it moves into the fixed die. The die wall friction prevents uniform pressure distribution. The compact has a higher density on top than on the bottom. In the latter type of pressing only the die is stationary in the press. Upper and lower punches advance simultaneously from above and below into the die (Figure 2.3). The consequence is high density at the top and undersides of the compact. In the centre there remains a ‘neutral zone’ which is relatively weak.

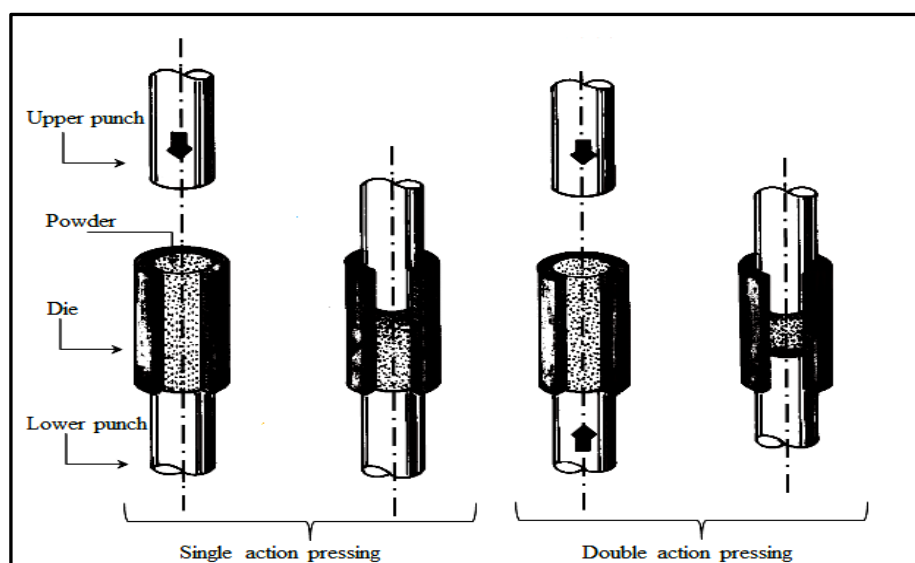


Figure 2.3: A schematic view of the events during die compaction of single and double action pressing (Upadhyaya, 2002)

## 2.5 Wetting angle and Capillary Force

In liquid phase sintering, the microstructure shows solid, liquid and vapour phase. The wetting angle formed by combination of liquid- solid and vapour is due to the molten metal on the substrate. The initial contact with the liquid phase is established by replacing the solid-gas interface through an equivalent interface of solid-liquid. The intensity of this interface substitution process is primarily governed by the wettability of the system (Kang, 2005). Contact angle plays a crucial role during the densification of the composite. Low contact angle helps in the liquid spreading over the solid grain particles homogeneously, thus pervasion a capillary attraction that assists densification system. Figure 2.4 shows contrast of wetting behaviour for a liquid on a horizontal plane showing how's the ability of the low-contact angle to support wetting whereas the high-contact angle resists wetting (Johnson and German, 1993). Densification requires a low-contact angle to ensure that the particles are pulled together. The wetting angle ( $\theta$ ) is associated with the balance of interfacial energy, and as follows Young's equation 2.1:

$$\gamma_{SV} = \gamma_{SL} + \gamma_{LV} \cos(\theta) \quad (2.1)$$

where  $\gamma_{SV}$  is the solid-vapour surface energy,  $\gamma_{SL}$  is the solid-liquid surface energy,  $\gamma_{LV}$  is the liquid-vapour surface energy and  $\theta$  is the contact angle. Usually, a small contact angle means good spread of liquid phase on the solid phase (Johnson and German, 1993).

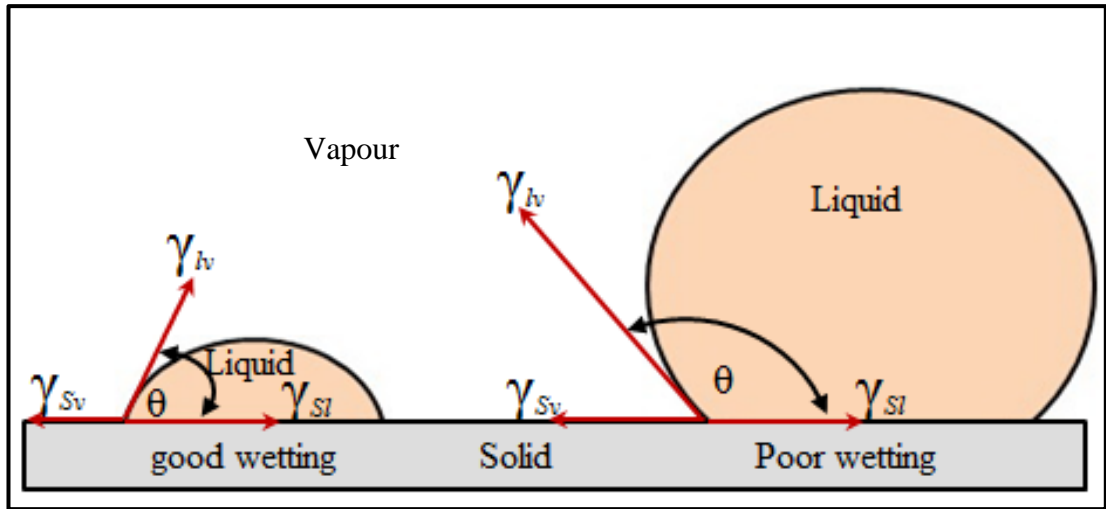


Figure 2.4: Wetting behaviour for a liquid on a horizontal plane (Johnson and German, 1993)

The primary objective in synthesizing composites is to combine two or more chemically and physically different material. The interfacing between the surfaces of different elements is very important (Laurent et al., 1987). That is why, when the contact angle decreased, the wettability enhanced resulting in significant improvement in densification in liquid phase sintering as well as the bonding. Surface purity is vital factor for interfacial energy, thus the wetting behaviour is radically distorted by contamination. Therefore, in metal-metal systems, the surface cleanliness is important and the sintering atmosphere plays a critical role on the densification of W-Cu composites. With less reactive metal powders, high vacuum or a reducing atmosphere is necessary to break down the surface oxide to achieve good wetting.

The primary powder mixtures are not in chemical equilibrium at sintering temperature in early stages, and chemical driving forces are also present. Due to the very low stresses required for activating the liquid flow, capillary forces play the most important role in the system of equilibrium or non-equilibrium. The processes

of shrinkage occur during isothermal liquid state sintering. These processes are usually divided into three stages as explained in section (2.5.2).

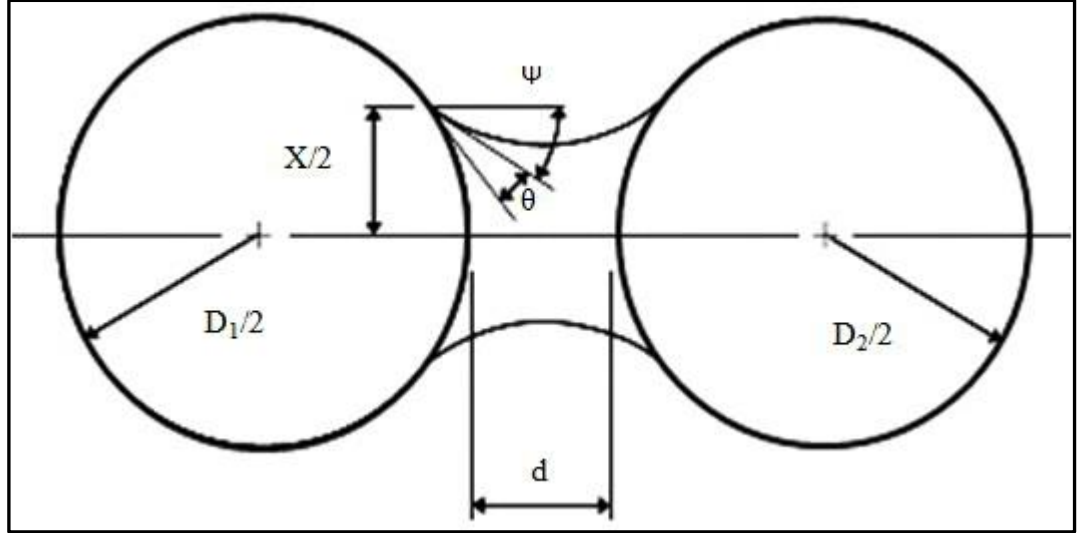


Figure 2.5: A schematic of two spheres of size  $D_1$  and  $D_2$  with a connecting liquid bridge. This geometry is used to calculate the capillary force responsible for rearrangement during LPS (German et al., 2009)

Particle rearrangement occurs by liquid flow and it is retarded by friction between the solid particles. Therefore, this stage requires good wetting since capillary forces acting at the liquid bridge are determined by the wetting angle. Fig.2.5 represents schematic of two spherical particles in size  $D_1$  and  $D_2$ , which connects the liquid bridge in thickness of  $d$ . The capillary force occurs as of the liquid-vapour surface tension. The total force between two particles is the sum of surface tension Eq: 2.2 and capillary force Eq: 2.3 (Qu et al., 2011).

$$F_{surface\ tension} = \gamma_{lv}\pi X \cos(\alpha) \quad (2.2)$$

$$F_{capillary} = \gamma_{lv} \left( \frac{1}{r} - \frac{2}{X} \right) \frac{\pi X^2}{4} \quad (2.3)$$

where  $\gamma_{lv}$  is the liquid-vapour surface energy,  $r$  and  $x/2$  are the principal radii of curvature,  $d$  is the inter-particle distance,  $\theta$  is the contact angle and  $\alpha$  is the angle depicted in Figure 2.5

In general full-density of W-Cu composites fabricated by LPS or liquid infiltration techniques is a complicated procedure. In this system, many parameters such as particle size of powder, type of mixing, green density, heating rate, holding time, cooling rate and environmental furnace affect the densification process. Suitably chosen parameters from these can reactively aid the sintered compact. Microstructures, mechanical and physical properties of W-Cu composites are affected by structure parameters for instance dihedral angle, connectivity and contiguity.

## 2.6 Dihedral angle and Contiguity

The angle between two particles is known as dihedral angle, which is shown in Fig. 2.6. The dihedral angle for a solid-liquid system is evident by the grain boundary groove that forms where the boundary emerges into the liquid. The lower portion of the figure shows the vector equilibrium which was used to link surface energies to the dihedral angle. It is described as the energy ratio between solid-liquid surface and grain boundaries. The angle at the junction between two particles is indicated as the dihedral angle, and if the interfacial tensions are in equilibrium at this junction then the interfacial tension is represented by Eq. 2.4 (German et al., 2009).

$$\gamma_{SS} = 2 \gamma_{SL} \cos \frac{\theta}{2} \quad (2.4)$$



where  $\gamma_{SS}$  is the grain boundary energy of solid-solid interface,  $\gamma_{SL}$  is the solid-liquid interfacial energy and  $\varphi$  is the dihedral angle. If the solid phase is amorphous, then there is no dihedral angle.

Contiguity ( $C_{SS}$ ) is the relative interface area of solid–solid bonds as a fraction of the total interfacial area of microstructure. Typically, contiguity is measured in two dimensions by quantitative microscopy based on the number of intercepts per unit length of test line according to Eq: 2.5.

$$C_{SS} = \frac{2N_{SS}}{2N_{SS} + N_{SL}} \quad (2.5)$$

where  $C_{SS}$  is the contiguity,  $N_{SS}$  is the solid-solid intercepts and  $N_{SL}$  is the solid-liquid intercepts. The contiguity is affected by volume content of solid phase and dihedral angle. Moreover, increase in the sintering time also results in the decrease of the contiguity (German, 1985a).

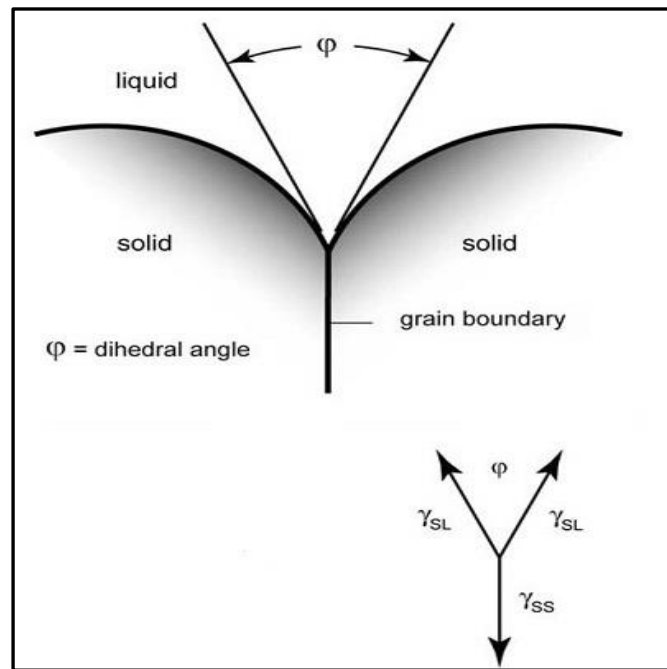


Figure 2.6: The dihedral angle for a solid-liquid system (German et al., 2009)

The value of contiguity plays a crucial role for mechanical and physical properties of composites. Numerous studies have attempted to explain the effect of contiguity on mechanical and physical properties. Wang and Hwang, (1998) examined the influence of the particle size of tungsten on processing parameter of infiltrated compact. They observed that, there is W-W contiguity affecting electrical properties such as electrical resistivity and thermal expansion coefficients of W-Cu composites. Lee et al., (2006) evaluated the conductivity in W-Cu system by applying the topological microstructures estimation. They concluded that, when the W-W contiguity increases, then the relative conductivity decreases. Recently, Çalışkan et al., (2013) reported that, the high value of contiguity affected mechanical properties such as tensile strength and ductility of 90W-7Ni-3Fe alloys.

## **2.7 Distortion**

The majority of sintering distortion has its basis in the compaction step or forming, and a significant sintering distortion amount is traced to the variation of green mass. The differences in density of composite compact powders are another reason of causing distortion. Higher sintering temperatures tend to cause a change in dimensions of the compact, both factors amplifying the gradients of green density. For this reason, in powder metallurgy selection of appropriate sintered density is very important to hinder the distortion during consolidation of the powder compact.

Liquid phase sintering is generally used in industry for net-shape production, but it is strictly limited to high solid content composites due to shape retention difficulties (German, 1985b). In tungsten-copper composites and tungsten heavy alloy, the large density difference (more than  $10\text{g/cm}^3$ ) between tungsten and matrix

and high content of liquid more than 25% vol., lead to significant distortion of the composites. (Upadhyaya and German, 1998; Binet et al., 2004 and Lu et al., 2001b).

A study by Wu et al., (2003) involved comparison of the distortion and densification behaviours of 80W-14Ni-6Fe and 80W-14Ni-6Cu heavy alloys. They stated that, prolonging sintering will lead to distortion. They also concluded that, firstly densification takes place and next the distortion occurs resulting in the loss of structural rigidity. This view is also supported by Yi et al., (2001) who also stated that, densification occurs first and then the distortion takes place. Lu et al., (2001b) concluded from their study that, as sintering time increases the distortion trend continues. They also observed that, the fraction of solid volume, the initial porosity and dihedral angle are important factors that control densification and distortion during liquid phase sintering.

## **2.8 Sintering categories**

Sintering is a processing technique used for bonding particles together at high temperature. The sintering process can be divided into two kinds: solid-state sintering (SSS) and liquid phase sintering (LPS). The solid state sintering occurs at temperatures less than the melting point of powder compacts, with the densification being achieved in solid state. Fig. 2.7 shows the schematic diagram of two different phases (Kang, 2005). It can be seen from the figure that solid state sintering of compact powder of A and B as composition  $X_1$  occur at  $T_1$ , while liquid phase sintering for same composition occurs at  $T_3$ . In addition, viscous flow sintering and transient liquid phase sintering can also be developed during sintering process as shown in Figure 2.7. When a high volume fraction of liquid is present the

densification of sintered compact can be achieved by viscous flow sintering. Besides, for a combination of solid-state sintering and liquid phase sintering, densification can be achieved by transient liquid phase sintering.

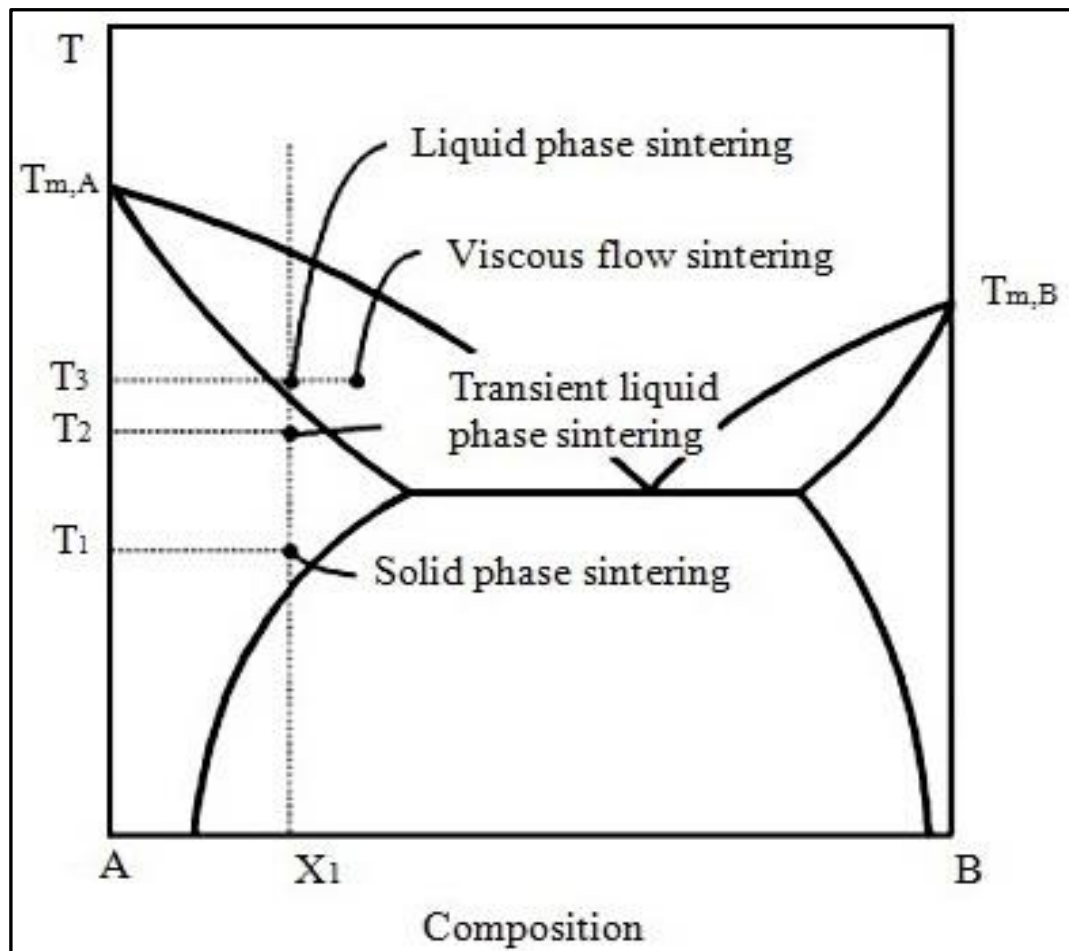


Figure 2.7: Illustrates different types of sintering (Kang, 2005)

### 2.8.1 Solid state sintering (SSS)

In the plurality of this technique, compacted powder are consolidated at temperature less than melting point of elements in order to provide the desirable mechanical and physical properties. Surface energy (capillary force) is the fundamental property facilitating the materials transport. Mechanism of material